Correspondence to:
Professor W. Henderson,
Department of Chemistry,
University of Waikato,
Private Bag 3105,
Hamilton,
New Zealand
e-mail: w.henderson@waikato.ac.nz
FAX: 0064-7-838-4219

Further studies on the dialkylation chemistry of $[Pt_2(\mu\text{-}S)_2(PPh_3)_4]$ with activated alkyl halides $RC(O)CH_2X$ (X = Cl, Br)

Oguejiofo T. Ujam[a], William Henderson[a,*], Brian K. Nicholson[a], and T. S. Andy Hor[b]

[a]*Department of Chemistry, University of Waikato, Private Bag 3105, Hamilton 3240, New Zealand*

[b]*Department of Chemistry, National University of Singapore, 3 Science Drive 3, Singapore 117543*

Received

Abstract

Further studies have been carried out into the reactivity of $[Pt_2(\mu\text{-}S)_2(PPh_3)_4]$ towards a range of activated alkylating agents of the type $RC(O)CH_2X$ (R = organic moiety e.g. phenyl, pyrenyl; X = Cl, Br). Alkylation of both sulfide centres is observed for $PhC(O)CH_2Br$, 3-(bromoacetyl)coumarin [$CouC(O)CH_2Br$], and 1-(bromoacetyl)pyrene [$PyrC(O)CH_2Br$], giving dications $[Pt_2\{\mu\text{-}SCH_2C(O)R\}_2(PPh_3)_4]^{2+}$, isolated as their PF_6^- salts. The X-ray structure of $[Pt_2\{\mu\text{-}SCH_2C(O)Ph\}_2(PPh_3)_4](PF_6)_2$ shows the presence of short Pt···O contacts. In contrast, the corresponding chloro compounds [typified by $PhC(O)CH_2Cl$] and imino analogues [e.g. $PhC(NOH)CH_2Br$] do not dialkylate $[Pt_2(\mu\text{-}S)_2(PPh_3)_4]$. The ability of $PhC(O)CH_2Br$ to dialkylate $[Pt_2(\mu\text{-}S)_2(PPh_3)_4]$ allows the synthesis of new mixed-alkyl dithiolate derivatives of the type $[Pt_2\{\mu\text{-}SCH_2C(O)Ph\}(\mu\text{-}SR)(PPh_3)_4]^{2+}$ (R = Et or n-Bu), through alkylation of *in situ*-generated monoalkylated compounds $[Pt_2(\mu\text{-}S)(\mu\text{-}SR)(PPh_3)_4]^+$ (from $[Pt_2(\mu\text{-}S)_2(PPh_3)_4]$ and excess RBr). In these heterodialkylated systems ligand replacement of PPh_3 occurs by the bromide ions in the reaction mixture forming monocations $[Pt_2\{\mu\text{-}SCH_2C(O)Ph\}(\mu\text{-}SR)(PPh_3)_3Br]^+$. This ligand substitution can be easily suppressed by addition of PPh_3 to the reaction mixture. The complex $[Pt_2\{\mu\text{-}SCH_2C(O)Ph\}(\mu\text{-}SBu)(PPh_3)_4]^{2+}$ was crystallographically characterised. X-ray crystal structures of the bromide-containing complexes $[Pt_2\{\mu\text{-}SCH_2C(O)Ph\}(\mu\text{-}SR)(PPh_3)_3Br]^+$ (R = Et, Bu) are also reported. In both structures the coordinated bromide is *trans* to the $SCH_2C(O)Ph$ ligand, which adopts an axial position, while the ethyl and butyl substituents adopt equatorial positions, in contrast to the structures of the dialkylated complexes $[Pt_2\{\mu\text{-}SCH_2C(O)Ph\}_2(PPh_3)_4]^{2+}$ and $[Pt_2\{\mu\text{-}SCH_2C(O)Ph\}(\mu\text{-}SBu)(PPh_3)_4]^{2+}$ (and many other known analogues) where both alkyl groups adopt axial positions.

Keywords: Dinuclear platinum complexes; Thiolate complexes; Alkylation reactions; Ligand substitution; Electrospray ionisation mass spectrometry; X-ray crystal structures

Introduction

Since the early discoveries of the nucleophilic nature of the platinum(II) sulfide complex $[Pt_2(\mu\text{-}S)_2(PPh_3)_4]$ **1** [1,2,3,4] there have been extensive studies into the chemistry of this versatile complex and analogous complexes with $\{Pt_2S_2\}$,[5,6,7] $\{Pt_2Se_2\}$ [8] and $\{Pd_2S_2\}$ [9,10] cores. There is particular interest in the alkylation [11,12,13,14,15,16] and arylation [17,18] chemistry of $\{Pt_2S_2\}$ complexes, and the alkylation of $\{Pt_2Se_2\}$ complexes,[19,20] because of the significant potential to synthesise novel thiolate (or selenolate) complexes using suitable organic electrophiles. The products formed with organic electrophiles are very much dependent on the nature of the electrophile. For simple monofunctional electrophiles, alkylation of one sulfide centre is most common,[21,22] but dialkylation can also occur, depending on the strength of the alkylating agent and the ancillary phosphine ligand on the $\{Pt_2S_2\}$ core.[23] Dialkylating agents produce either monoalkylated, cyclised or bridged products depending on the alkylating agent and experimental conditions,[24,25,26] including the use of high-pressure syntheses.[27] Of particular note is the ability to stepwise introduce two different organic groups on the $\{Pt_2S_2\}$ core, resulting in the formation of dinuclear mixed-thiolate complexes $[Pt_2(\mu\text{-}SR^1)(\mu\text{-}SR^2)(PPh_3)_4]^{2+}$ not easily accessible by other routes.[28] However, the alkylation of a monocationic $[Pt_2(\mu\text{-}S)(\mu\text{-}SR)(PPh_3)_4]^{+}$ complex requires a powerful alkylating agent (Me_2SO_4) that generates a non-nucleophilic anion ($MeSO_4^-$) due to the susceptibility of the dications $[Pt_2(\mu\text{-}SR^1)(\mu\text{-}SR^2)(PPh_3)_4]^{2+}$ to nucleophilic attack by anions such as iodide (generated from alkyl iodide electrophiles).[14] The use of diphosphines and high-pressure conditions does allow heterodialkylation with a range of substrates, but such conditions are not necessarily convenient.[29]

We wished to extend the heterodialkylation methodology more widely, as well as better understand the factors that promote dialkylation, and in this paper we report on further

studies on the dialkylation chemistry of $[Pt_2(\mu\text{-}S)_2(PPh_3)_4]$ **1** towards electrophiles of the type $RC(O)CH_2X$ (X = Cl or Br).

Results and discussion

Previously it has been found that reaction of $[Pt_2(\mu\text{-}S)_2(PPh_3)_4]$ **1** with $PhC(O)CH_2Cl$ yields the monoalkylated complex $[Pt_2(\mu\text{-}S)\{\mu\text{-}SCH_2C(O)Ph\}(PPh_3)_4]^+$ **2**.[22] Reaction of **1** with a large excess (10 mole equivalents) of $PhC(O)CH_2Cl$ in methanol, initially stirred at room temperature for 48 h and then refluxed for 24 h, did not result in dialkylation, with the monoalkylated product only being recovered. However, reaction of **1** with a large excess of the corresponding bromide $PhC(O)CH_2Br$ at room temperature proceeded much more rapidly, giving complete conversion to the monoalkylated complex in less than 5 minutes, followed by a somewhat slower conversion to the dialkylated complex $[Pt_2\{\mu\text{-}SCH_2C(O)Ph\}_2(PPh_3)_4]^{2+}$ **3**. The rate of alkylation of the free sulfide in monoalkylated complexes $[Pt_2(\mu\text{-}S)(\mu\text{-}SR)(PPh_3)_4]^+$ is notably slower than the alkylation of **1** itself, due to the positive charge on the complex and steric shielding of the residual free sulfide ligand. Positive ion ESI mass spectrometry was used as a convenient technique for monitoring the progress of the alkylation reactions, with the monoalkylated and dialkylated cations giving distinctive peaks at *m/z* 1621 and 870 respectively. The complex was isolated as its hexafluorophosphate salt $\mathbf{3}\cdot(PF_6)_2$ by addition of excess NH_4PF_6 to the reaction mixture. It is noteworthy that in the synthesis of this complex there was no indication of any secondary product formed by ligand substitution of PPh_3 by bromide, as is seen in other related systems (*vide infra*). Consistent with its symmetric nature, complex $\mathbf{3}\cdot(PF_6)_2$ has a single resonance in its $^{31}P\{^1H\}$ NMR spectrum at δ 20.1 showing $^1J(PtP)$ coupling of 3128 Hz.

Other $RC(O)CH_2Br$ compounds also effected dialkylation of **1**. 1-(Bromoacetyl)pyrene, $PyrC(O)CH_2Br$ **4** formed $[Pt_2\{\mu\text{-}SCH_2C(O)Pyr\}_2(PPh_3)_4]^{2+}$ **5** (*m/z* 996)

after stirring for 7 days; the reduced reactivity in this case is expected to be due to the greater steric bulk of the pyrene group compared to a single phenyl ring. An additional minor ion at *m/z* 1748 in this reaction mixture is from the monoalkylated complex $[Pt_2(\mu\text{-}S)\{\mu\text{-}SCH_2C(O)Pyr\}(PPh_3)_4]^+$. 3-(Bromoacetyl)coumarin, $CouC(O)CH_2Br$ **6** reacted with **1** to form predominantly $[Pt_2\{\mu\text{-}SCH_2C(O)Cou\}_2(PPh_3)_4]^{2+}$ **7** (*m/z* 939) after 7 days at room temperature, together with about 5% of the monoalkylated product $[Pt_2(\mu\text{-}S)\{\mu\text{-}SCH_2C(O)Cou\}(PPh_3)_4]^+$ (*m/z* 1697). Prolonged reaction (to try and drive the reaction to completion) resulted in significant decomposition occurring. Several attempts at repeating the reaction to obtain a purer product gave similar results, but with different impurity species, presumably due to various secondary reactions. Complexes **5** and **7** were isolated as their hexafluorophosphate salts $\mathbf{5}\cdot(PF_6)_2$ and $\mathbf{7}\cdot(PF_6)_2$ by addition of excess NH_4PF_6 to the reaction mixtures. While $\mathbf{7}\cdot(PF_6)_2$ gave satisfactory elemental microanalyses, the sample was impure, as shown by ESI MS and ^{31}P NMR.

The ability of $PhC(O)CH_2Br$ to dialkylate $[Pt_2(\mu\text{-}S)_2(PPh_3)_4]$ suggested that it would provide a complementary alkylating agent to Me_2SO_4 for the alkylation of monoalkylated complexes $[Pt_2(\mu\text{-}S)(\mu\text{-}SR)(PPh_3)_4]^+$, generating a new series of mixed-alkyl dithiolate complexes $[Pt_2\{\mu\text{-}SC(O)Ph\}(\mu\text{-}SR)(PPh_3)_4]^{2+}$. Monoalkylated complexes $[Pt_2(\mu\text{-}S)(\mu\text{-}SR)(PPh_3)_4]^+$ (R = Et or n-Bu, hereafter Bu) were generated *in situ* by reaction of $[Pt_2(\mu\text{-}S)_2(PPh_3)_4]$ **1** with an excess of EtBr or BuBr in methanol, followed by removal of the excess alkylating agent by evaporation. These complexes were then redissolved in methanol and reacted with excess $PhC(O)CH_2Br$, and the reaction mixtures monitored by ESI MS. The alkylation of the free sulfide was fast, generating the hetero-dialkylated derivatives $[Pt_2\{\mu\text{-}SCH_2C(O)Ph\}(\mu\text{-}SR)(PPh_3)_4]^{2+}$ (**8**, R = Bu; **9**, R = Et), but their formation was followed by spontaneous substitution of one of the PPh_3 ligands by a bromide anion. At an intermediate stage in the reaction (6 hours), four major species were observed in the ESI mass spectrum of

the butyl system. These were $[Pt_2\{\mu\text{-}SCH_2C(O)Ph\}(\mu\text{-}SBu)(PPh_3)_4]^{2+}$ (*m/z* 839, 19%), $[Pt_2\{\mu\text{-}SCH_2C(O)Ph\}(\mu\text{-}SBu)(PPh_3)_3\text{-}H]^+$ (*m/z* 1415, 90%), $[Pt_2\{\mu\text{-}SCH_2C(O)Ph\}(\mu\text{-}SBu)(PPh_3)_3Br]^+$ **10** (*m/z* 1497, 40%), and $[Pt_2(\mu\text{-}S)(\mu\text{-}SBu)(PPh_3)_4]^+$ (*m/z* 1560, 100%). The species $[Pt_2\{\mu\text{-}SCH_2C(O)Ph\}(\mu\text{-}SBu)(PPh_3)_3\text{-}H]^+$ might be formed by deprotonation of the $C(O)CH_2$ group. After stirring for 48 h, the bromide-substituted complex $[Pt_2\{\mu\text{-}SCH_2C(O)Ph\}(\mu\text{-}SBu)(PPh_3)_3Br]^+$ was the major species, and was isolated as its hexafluorophosphate salt **10**·PF_6 by addition of excess NH_4PF_6. A similar result was obtained from the *in situ*-generated $[Pt_2(\mu\text{-}S)(\mu\text{-}SEt)(PPh_3)_4]^+$, which yielded $[Pt_2\{\mu\text{-}SCH_2C(O)Ph\}(\mu\text{-}SEt)(PPh_3)_3Br]PF_6$ **11**·PF_6 on reaction with excess $PhC(O)CH_2Br$ and precipitation with NH_4PF_6. The order of alkylation is important; to generate the heterodialkylated complexes it is necessary to retain the strongest alkylating agent for alkylation of the monoalkylated intermediate. Thus attempted reaction of $[Pt_2(\mu\text{-}S)\{\mu\text{-}SCH_2C(O)Ph\}(PPh_3)_4]^+$ with EtBr or BuBr gave no reaction.

The displacement of PPh_3 by bromide is promoted by the dicationic nature of the thiolate complexes, which makes them susceptible to nucleophilic attack by bromide, a moderately good nucleophile with a reasonable affinity for platinum(II). However it is noteworthy that this secondary reaction occurs for $[Pt_2\{\mu\text{-}SCH_2C(O)Ph\}(\mu\text{-}SBu)(PPh_3)_4]^{2+}$ **8**, but not for $[Pt_2\{\mu\text{-}SCH_2C(O)Ph\}_2(PPh_3)_4]^{2+}$ **3**, which is probably related to the significantly smaller size of ethyl and butyl groups which allows the incoming bromide nucleophile an easier pathway to attack the electrophilic platinum centre. This is supported by X-ray crystal structure determinations (*vide infra*).

In order to suppress the loss of triphenylphosphine to enable isolation of the $[Pt_2\{\mu\text{-}SCH_2C(O)Ph\}(\mu\text{-}SR)(PPh_3)_4]^{2+}$ (R = Et, Bu) cations **8** and **9**, the syntheses were repeated with the addition of 1 mole equivalent of PPh_3 following formation of the ions $[Pt_2\{\mu\text{-}$

$SCH_2C(O)Ph\}(\mu\text{-}SR)(PPh_3)_3Br]^+$. This resulted in good conversion to the $[Pt_2\{\mu\text{-}SCH_2C(O)Ph\}(\mu\text{-}SR)(PPh_3)_4]^{2+}$ ions which were isolated as hexafluorophosphate salts **8**·$(PF_6)_2$ and **9**·$(PF_6)_2$.

The reactivity of some related imine-containing alkylating agents of the type $RC(=NR')CH_2X$ (X = Cl, Br) towards **1** was also studied. However, these were incapable of dialkylating **1** under the conditions investigated, and therefore contrast markedly with $RC(O)CH_2Br$, which readily dialkylate **1**. For example, under relatively forcing reaction conditions (methanol reflux, 24 h), the oxime $PhC(=NOH)CH_2Br$ only monoalkylated **1**, giving the previously reported cation $[Pt_2(\mu\text{-}S)\{\mu\text{-}SCH_2C(=NOH)Ph\}(PPh_3)_4]^+$.[22] In this case, the lower electron-withdrawing effect of the oxime group (compared to a carbonyl in $PhC(O)CH_2Br$) makes the CH_2 carbon less electrophilic. Similarly, the semicarbazones $PhC\{=NNHC(O)NH_2\}CH_2Br$ and *p*-$PhC_6H_4C\{=NNHC(O)NH_2\}CH_2Br$ also only monoalkylated **1**, again giving previously reported derivatives.[22]

In order to investigate possible structural reasons for the observed reactivity towards phosphine substitution, and to fully characterise the bromide-substituted products, a number of single-crystal X-ray structure determinations were carried out. The structure of the cation of $[Pt_2\{\mu\text{-}SCH_2C(O)Ph\}_2(PPh_3)_4](PF_6)_2$ **3**·$(PF_6)_2$ is shown in Figure 1, while selected bond lengths and angles are given in Table 1. Attempts at obtaining suitable single crystals of the butylthiolate complex $[Pt_2\{\mu\text{-}SCH_2C(O)Ph\}(\mu\text{-}SBu)(PPh_3)_4](PF_6)_2$ **8**·$(PF_6)_2$ were unsuccessful, but crystals of the corresponding tetraphenylborate complex **8**·$(BPh_4)_2$ were able to be obtained. The structure of the cation is shown in Figure 2, with selected bond lengths and angles in Table 2. In both structures, the thiolate ligands adopt axial positions on the $\{Pt_2S_2\}$ butterfly core, an arrangement which minimises steric interactions with the bulky PPh_3 ligands (though at the expense of 1,3-diaxial interactions between the two thiolate ligands. Other dialkylated $\{Pt_2S_2\}$ complexes, such as $[Pt_2(\mu\text{-}SMe)_2(PPh_3)_4]^{2+}$ [28], $[Pt_2(\mu\text{-}$

SMe)(μ-SR)$(PPh_3)_4]^{2+}$ (R = CH_2Ph, $CH_2CH{=}CH_2$, $C_5H_{10}CO_2Et$, C_2H_4SPh) [28] and [Pt_2(μ-$SCH_2Ph)_2(dppp)_2]^{2+}$ [dppp = $Ph_2P(CH_2)_3PPh_2$] [23] also have the same arrangement.

The {Pt_2S_2} core of **3**·$(PF_6)_2$ has a dihedral angle (θ, between the two PtS_2 planes) of 156.36°, very similar to the corresponding angle in [Pt_2(μ-$SMe)_2(PPh_3)_4]^{2+}$ (156.87°).[28] The corresponding angle in **8**·$(BPh_4)_2$ is 145.11°. These dialkylated derivatives have considerably flatter {Pt_2S_2} butterfly cores (with larger θ values) when compared to monoalkylated derivatives such as [Pt_2(μ-S){μ-$SCH_2C(O)Ph$}$(PPh_3)_4]^+$ (134.71°).[22] The Pt-P bond distances of complex **3**·$(PF_6)_2$ range from 2.2703(19) to 2.2902(14) Å. The carbonyl oxygen atoms reside above the Pt centres [Pt(1)···O(2) 2.711, Pt(2)···O(1) 2.901 Å, though there is some disorder in the Pt(2) position so this value may be less reliable]. This may represent an interaction, since the sum of the van der Waals radii for Pt and O is 3.24 Å.[30] In monoalkylated [Pt_2(μ-S){μ-$SCH_2C(O)Ph$}$(PPh_3)_4]^+$ the C=O group also resides approximately above the Pt centre, but the Pt···O distance is a lot longer (3.604 Å). The Pt centres in **3**·$(PF_6)_2$ are expected to be more electrophilic than in [Pt_2(μ-S){μ-$SCH_2C(O)Ph$}$(PPh_3)_4]^+$, as a result of the dipositive charge on the complex which would promote a stronger Pt···O interaction compared to the monoalkylated complex.

The mixed-thiolate complex **8**·$(BPh_4)_2$ shows overall similar features; again the carbonyl oxygen sits above the Pt centre with a fairly short Pt···O distance of 2.981 Å. The butyl group however takes up a position pointing away from the platinum atoms. The Pt-P bonds *trans* to the SBu ligand [Pt(1)-P(2) 2.321(3), Pt(2)-P(3) 2.303(3) Å] are longer than those *trans* to the phenacylthiolate ligand [Pt(1)-P(1) 2.294(3), Pt(2)-P(4) 2.284(3) Å], indicating that the SBu ligand has a higher *trans* influence.[31] This is in accord with $^{31}P\{^1H\}$ NMR spectroscopic measurements; the ^1J(PtP) values of PPh_3 ligands *trans* to SBu and SCH_2COPh ligands in complexes [Pt_2(μ-S)(μ-$SR)(PPh_3)_4]^+$ [22, 32] are 3235 and 3386 Hz respectively.

The structures of **3**·$(PF_6)_2$ and **8**·$(BPh_4)_2$ provide an explanation as to why bromide-substituted products are not formed when both thiolate ligands are $SCH_2C(O)Ph$. The presence of the carbonyl groups in close proximity to both Pt centres in **3** sterically protects them towards attack by bromide ions. However in **8**, while one of the Pt centres [Pt(2)] is similarly protected by a C(O)Ph group, the other platinum Pt(1) is more exposed, offering a pathway to bromide attack, consistent with the observed formation of bromide-substituted products in the case of $[Pt_2\{\mu\text{-}SCH_2C(O)Ph\}(\mu\text{-}SR)(PPh_3)_4]^{2+}$ (R = Bu or Et).

The structures of the bromide-substituted complexes $[Pt_2\{\mu\text{-}SCH_2C(O)Ph\}(\mu\text{-}SBu)(PPh_3)_3Br]PF_6$ **10**·PF_6 and $[Pt_2\{\mu\text{-}SCH_2C(O)Ph\}(\mu\text{-}SEt)(PPh_3)_3Br]PF_6$ **11**·PF_6 were also determined, and are shown in Figures 3 and 4 respectively. Selected bond lengths and angles are given in Tables 3 and 4. The two structures are isomorphous, despite the different alkyl substituents. There are some significant differences between the bromide-containing complexes and their 'parent' triphenylphosphine analogues **3** and **8**, as can be seen in the Figures and Table 5, which shows a comparison of selected parameters of the $\{Pt_2S_2\}$ cores of complexes **3**, **8**, **10** and **11**.

Complexes **10** and **11** have a significantly more folded $\{Pt_2S_2\}$ butterfly core, with dihedral angles between the two PtS_2 planes [**10** 124.66, **11** 123.84°] that are substantially smaller than in the corresponding non-bromide complexes **3** and **8** (*vide supra*). This results in a marked shortening of the transannular distances. For example the Pt···Pt and S···S separations in **10** [3.2197(4) and 2.979(3) Å respectively] are significantly less than the corresponding values in **8** [3.4159(4) and 3.107(4) Å]. The Pt-S-Pt angles are also decreased in **10** and **11** (Table 5). In **10** and **11** the phenacylthiolate ligands adopt axial positions, but, significantly, the butyl and ethyl substituents both adopt *equatorial* positions. Most likely this is due to the presence of the smaller bromide ligand, which opens up a pocket of space in the equatorial plane, in which the ethyl or butyl substituent can reside, with concomitant

increased puckering of the $\{Pt_2S_2\}$ core to accommodate the steric bulk of the remaining groups.

Examination of the Cambridge Structural Database (version 5.32, February 2011 update) for complexes of the type $P_2Pt(\mu\text{-}SR)_2PtP_2$ (P = phosphine ligand, R = organic substituent) reveals that, of those complexes with puckered $\{Pt_2S_2\}$ cores, in all cases the thiolate ligands both adopt axial (*syn*) positions [some structures, having planar $\{Pt_2S_2\}$ cores, e.g. $[dpppPt(\mu\text{-}SCH_2CH_2NHC(O)NHPh)_2Pt(dppp)](CF_3SO_3)_2$ [33] have an *anti* arrangement of the thiolate ligands across the core]. Although there are no known structures of derivatives with a single halide (X) replacing a phosphine ligand (P), *viz*. $P_2Pt(\mu\text{-}SR)_2PtXP$, there are several structures containing cations of the type **12**.[4,34,35,36] In these, the SR group on the phosphine side of the $\{Pt_2S_2\}$ core adopts an axial position, while the other (on the side of the smaller anionic ligand, e.g. halide) is in an equatorial position, similar to the arrangement in **10** and **11**. The complex $(Ph_3P)BrPt(\mu\text{-}SMe)_2PtBr(PPh_3)$ **12d** [36] provides the closest comparison to **10** and **11**; in this complex the $\{Pt_2S_2\}$ core is also significantly puckered (θ = 129.19°), though less puckered than **10** and **11** (which have dihedral angles *ca.* 124°, Table 5). Concomitantly, the Pt···Pt separation in **12d** [3.247 Å] is larger than **10** and **11**. A detailed theoretical study on dinuclear Pt complexes with thiolate bridges has found that energy differences between different arrangements in these systems is small.[37]

In complex **10**, and especially in the ethylthiolate **11**, the C(O)Ph group is not located directly above a platinum centre; these complexes are monocationic, the Pt centres are presumably less electrophilic, and there is no Pt···O interaction, as is the case for $[Pt_2(\mu\text{-}S)\{\mu\text{-}SCH_2C(O)Ph\}(PPh_3)_4]^+$. Both **10** and **11** have the coordinated bromide ligand *trans* to the $SCH_2C(O)Ph$ ligand. In complex **10** the Pt-P bond distances for the phosphines *trans* to the SBu ligand are similar [Pt(1)-P(1) 2.268(2) and Pt(2)-P(2) 2.270(2) Å], both being shorter than the Pt(2)-P(3) bond *trans* to $SCH_2C(O)Ph$, the opposite trend to that observed in the non-

bromide complex **8**. The same effect is observed in **11**. The lower *trans* influence of bromide compared to PPh_3 can be seen in complexes **10** and **11**, with the Pt(2)-S(1) bond length (of e.g. **11**) [2.2799(11) Å] shorter than Pt(1)-S(1) [2.3655(10) Å].

The phosphine complexes $[Pt_2\{\mu\text{-}SCH_2C(O)Ph\}(\mu\text{-}SR)(PPh_3)_4](PF_6)_2$ **3** and **8** show a single resonance in their $^{31}P\{^1H\}$ NMR spectra due to almost coincidental phosphine chemical shifts (which could not be resolved by the use of other solvents e.g. d^6-DMSO), but two sets of ^{195}Pt satellites are observed for the phosphines *trans* to the two different thiolate ligands, with coupling constants of 3107 and 2934 Hz in **8**. The behaviour shown by the bromide complexes $[Pt_2\{\mu\text{-}SCH_2C(O)Ph\}(\mu\text{-}SR)(PPh_3)_3Br]PF_6$ **10** and **11** was more complicated. If the structures observed in the solid state were maintained in solution, three different PPh_3 environments, and hence a relatively simple spectrum would be observed. The ^{31}P NMR spectrum of $[Pt_2\{\mu\text{-}SCH_2C(O)Ph\}(\mu\text{-}SBu)(PPh_3)_3Br]PF_6$ **10**$\cdot PF_6$ showed several (> 4, possibly 6) overlapping multiplets with their corresponding ^{195}Pt satellites, which may arise from the presence of isomers in solution. This may be due to axial/equatorial conversion of the SBu group, or alternatively it is possible that geometric isomers are formed, with the bromide *trans* to either SBu or SCH_2COPh, and that the crystal selected for X-ray crystallographic study is one of these isomers.

Conclusions

In this work we have demonstrated that phenacyl bromide $[PhC(O)CH_2Br]$ (but not imine derivatives thereof), and other compounds of the type $RC(O)CH_2Br$ [3-(bromoacetyl)coumarin and 1-(bromoacetyl)pyrene] successfully dialkylate $[Pt_2(\mu\text{-}S)_2(PPh_3)_4]$ **1** and monoalkylated derivatives $[Pt_2(\mu\text{-}S)(\mu\text{-}SR)(PPh_3)_4]^+$, leading to new hetero-dithiolate platinum complexes. X-ray structure determinations suggest a Pt···O=C interaction in the dicationic, dialkylated complexes $[Pt_2\{\mu\text{-}SCH_2C(O)Ph\}_2(PPh_3)_4](PF_6)_2$ **3**$\cdot(PF_6)_2$ and

$[Pt_2\{\mu\text{-}SCH_2C(O)Ph\}(\mu\text{-}SBu)(PPh_3)_4](BPh_4)_2$ **8**·$(BPh_4)_2$. When one of the thiolate ligands contains ethyl or n-butyl, attack of the liberated bromide anion results in phosphine substitution giving mono-cationic complexes $[Pt_2\{\mu\text{-}SC(O)Ph\}(\mu\text{-}SR)(PPh_3)_3Br]^+$ (R = Et or Bu). This process can be successfully suppressed by simply adding PPh_3 to the reaction mixture at the completion of the alkylation reactions. With these results, we now have a greater understanding of factors that influence the dialkylation of **1**, and the products that are formed.

Experimental

The complex $[Pt_2(\mu\text{-}S)_2(PPh_3)_4]$ **1** was prepared by the literature procedure from *cis*-$[PtCl_2(PPh_3)_2]$ and $Na_2S{\cdot}9H_2O$ in benzene.[2,38] The following compounds were used as supplied from commercial sources: phenacyl chloride (BDH), phenacyl bromide (Aldrich), 1-bromobutane (BDH), bromoethane (BDH), 1-(bromoacetyl)pyrene (Aldrich), 3-(bromoacetyl)coumarin (Aldrich), sodium tetraphenylborate (Aldrich), triphenylphosphine (BDH) and ammonium hexafluorophosphate (Aldrich). Reactions were carried out in LR grade methanol, without precautions to exclude light, air or moisture. Water was singly distilled prior to use.

^1H NMR spectra were recorded on Bruker DRX spectrometers operating either at 300 or 400 MHz. $^{31}P\{^1H\}$ NMR spectra were recorded on a Bruker DRX spectrometer operating at 121.49 MHz. Spectra were recorded in CD_2Cl_2 solution; all dialkylated complexes had relatively poor solubility in $CDCl_3$. ESI mass spectra were recorded on a VG Platform II instrument; samples were prepared by dissolving a small quantity (< 1 mg) of sample in a few drops of CH_2Cl_2 and diluting with methanol. Cone voltages were typically 20 V. High resolution mass spectra were recorded on a Bruker MicrOTOF instrument. Assignment of ions was achieved by use of a simulation program.[39,40] Melting points were recorded on a

Reichert Thermovar hotstage apparatus and are uncorrected. Infrared spectra were recorded as KBr discs on a Perkin Elmer Spectrum 100 FTIR spectrometer and microelemental analyses were carried out at the Campbell Microanalytical Laboratory at the University of Otago.

Synthesis of $[Pt_2\{\mu\text{-}SCH_2C(O)Ph\}_2(PPh_3)_4](PF_6)_2$ $\mathbf{3}\cdot(PF_6)_2$

To a suspension of $[Pt_2(\mu\text{-}S)_2(PPh_3)_4]$ (100 mg, 0.067 mmol) in methanol (30 mL) was added $PhC(O)CH_2Br$ (132.4 mg, 0.67 mmol) and the mixture stirred at room temperature. After 1 h a clear pale yellow solution had formed. After 24 h the nearly colourless solution was analysed by ESI MS and found to contain solely $[Pt_2\{\mu\text{-}SCH_2C(O)Ph\}_2(PPh_3)_4]^{2+}$. After filtration to remove a trace amount of insoluble matter, solid NH_4PF_6 (80 mg, 0.49 mmol) was added, followed by water (30 mL) to induce precipitation. The solid was filtered and washed successively with water (10 mL), methanol (10 mL) and diethyl ether (10 mL) and dried under vacuum to give $\mathbf{3}\cdot(PF_6)_2$ as an off-white powder (90.5 mg, 67%). Found: C 51.77; H 3.69. $C_{88}H_{74}F_{12}O_2P_6Pt_2S_2$ (M_r 2030.49) requires C 52.01; H 3.67%. M.p. 221-223 °C. IR ν_{max} 1673 cm^{-1}. ESI MS *m/z* 870 (100%), $[Pt_2\{\mu\text{-}SCH_2C(O)Ph\}_2(PPh_3)_4]^{2+}$. $^{31}P\{^1H\}$ NMR, δ 20.1 [s, $^1J(PtP)$ 3128]. ^1H NMR (300 MHz), δ 2.11 (br s, 4H, CH_2), 7.06-7.79 (m, 70H, Ph).

Synthesis of $[Pt_2\{\mu\text{-}SCH_2C(O)Pyr\}_2(PPh_3)_4](PF_6)_2$ $\mathbf{5}\cdot(PF_6)_2$

A mixture of $[Pt_2(\mu\text{-}S)_2(PPh_3)_4]$ (100 mg, 0.067 mmol) and 1-(bromoacetyl)pyrene **4** (129 mg, 0.399 mmol) in methanol (25 mL) was stirred for 7 days. Complete formation of the product cation was shown by ESI MS. The solution was filtered to remove traces of insoluble impurities and excess NH_4PF_6 (40 mg, 0.245 mmol) added to the filtrate, giving a bright yellow precipitate. Distilled water (10 mL) was added to assist precipitation. The product was filtered, washed with water (40 mL), diethyl ether (40 mL) and dried under vacuum to give a

yellowish-orange powder of **5**·$(PF_6)_2$ (98 mg, 65%). Found: C 56.69; H 3.92. $C_{108}H_{82}F_{12}O_2P_6Pt_2S_2$ (M_r 2278.56) requires C 56.88; H 3.63%. M.p. 222-224 °C. IR ν_{max} 1638 cm^{-1}. ESI MS *m/z* 996 (100%), $[Pt_2\{\mu\text{-}SCH_2C(O)Pyr\}_2(PPh_3)_4]^{2+}$. $^{31}P\{^1H\}$ NMR, δ 22.4 [s, ^1J(PtP) 3136]. ^1H NMR (300 MHz), δ 2.47 (br s, 4H, SCH_2) and 6.68-8.45 (m, aromatic CH).

Synthesis of $[Pt_2\{\mu\text{-}SCH_2C(O)Cou\}_2(PPh_3)_4](PF_6)_2$ 7·$(PF_6)_2$

A mixture of $[Pt_2(\mu\text{-}S)_2(PPh_3)_4]$ (100 mg, 0.067 mmol) and 3-(bromoacetyl)coumarin **6** (107 mg, 0.401 mmol) in methanol (25 mL) was stirred for 7 days. After filtration to remove traces of insoluble matter excess NH_4PF_6 (40 mg, 0.245 mmol) was added, giving a white precipitate. Water (10 mL) was added to assist precipitation. The product was filtered, washed with water (40 mL), diethyl ether (40 mL) and dried under vacuum to give crude **7**·$(PF_6)_2$ (92 mg, 64%). Found: C 51.77; H 3.59. $C_{94}H_{74}F_{12}O_6P_6Pt_2S_2$ (M_r 2166.47) requires C 52.08; H 3.44. M.p. 178-180 °C. IR ν_{max} 1608, 1725 cm^{-1}. ESI MS *m/z* 938.151 (100%), $[Pt_2\{\mu\text{-}SCH_2C(O)Cou\}_2(PPh_3)_4]^{2+}$. $^{31}P\{^1H\}$ NMR, δ 18.9 [s, ^1J(PtP) 3110]. ^1H NMR (400 MHz), δ 3.52 [t, 4H, SCH_2, J(PH) 5.2, J(PtH) *ca.* 30] and 7.05-7.91 (m, aromatic CH).

Synthesis of $[Pt_2\{\mu\text{-}SCH_2C(O)Ph\}(\mu\text{-}SBu)(PPh_3)_4](PF_6)_2$ 8·$(PF_6)_2$

$[Pt_2(\mu\text{-}S)_2(PPh_3)_4]$ (100 mg, 0.067 mmol) was reacted with excess 1-bromobutane (1 mL, large excess) in methanol (25 mL), and the mixture stirred for 1 h to give a yellow solution. ESI MS indicated complete formation of $[Pt_2(\mu\text{-}S)(\mu\text{-}SBu)(PPh_3)_4]^+$. The volatiles were removed by rotary evaporation, and the residue redissolved in methanol (25 mL). $PhC(O)CH_2Br$ (66 mg, 0.34 mmol) was then added and the reaction mixture stirred overnight. Triphenylphosphine (17.5 mg, 0.067 mmol) was added, and the reaction mixture stirred an additional 12 h. The solution was filtered to remove traces of insoluble matter and excess

NH_4PF_6 (40 mg, 0.245 mmol) added, giving an off-white precipitate. Water (10 mL) was added to assist precipitation. The product was filtered, washed with water (40 mL) and diethyl ether (40 mL) and dried under vacuum to give **8**·$(PF_6)_2$ (69.5 mg, 53%). Found: C 51.08; H 3.89. $C_{84}H_{76}F_{12}OP_6Pt_2S_2$ (M_r 1968.52) requires C 51.22; H 3.89%. M.p. 188-191 °C. IR ν_{max} 1637 cm^{-1}. ESI MS *m/z* 839 (100%), $[Pt_2\{\mu\text{-}SCH_2C(O)Ph\}(\mu\text{-}SBu)(PPh_3)_4]^{2+}$. $^{31}P\{^1H\}$ NMR, δ 19.6 [br s, ^1J(PtP) 3107 and 2934]. ^1H NMR (400 MHz), δ 0.36 (m, 2H, CH_3), 0.55 (m, 2H, CH_2), -0.4 (m, 2H, CH_2), 2.06 (m, br, 2H, SCH_2), 2.7 (m, br, 2H, SCH_2), 7.08-7.77 (m, 65H, Ph).

Attempts at obtaining single crystals of this compound suitable for an X-ray diffraction study were unsuccessful. The corresponding BPh_4^- salt was prepared in an analogous manner (replacing NH_4PF_6 by $NaBPh_4$) and yielded suitable crystals by vapour diffusion of diethyl ether into a dichloromethane solution of the complex.

Synthesis of $[Pt_2\{\mu\text{-}SCH_2C(O)Ph\}(\mu\text{-}SEt)(PPh_3)_4](PF_6)_2$ 9·$(PF_6)_2$

Following the procedure for **8**·$(PF_6)_2$, $[Pt_2(\mu\text{-}S)_2(PPh_3)_4]$ (100 mg, 0.067 mmol) in methanol (25 mL) with bromoethane (1 mL, large excess) formed the monoalkylated complex $[Pt_2(\mu\text{-}S)(\mu\text{-}SEt)(PPh_3)_4]^+$. The resulting yellow solution was reacted with $PhC(O)CH_2Br$ (66 mg, 0.34 mmol) and then PPh_3 (17.5 mg, 0.067 mmol), followed by precipitation of the product with NH_4PF_6 (40 mg, 0.245 mmol). The product was filtered, washed with water (2 x 20 mL) and diethyl ether (2 x 20 mL) and dried under vacuum to give **9**·$(PF_6)_2$ (74 mg, 57%) as a white powder. Found: C 50.53; H 3.65. $C_{82}H_{72}F_{12}OP_6Pt_2S_2$ (M_r 1940.48) requires C 50.73; H 3.74%. M.p. 211-213 °C. IR ν_{max} 836, 1096, 1436, 1481, 1674 cm^{-1}. ESI MS *m/z* 826 (100%), $[Pt_2\{\mu\text{-}SCH_2C(O)Ph\}(\mu\text{-}SEt)(PPh_3)_4]^{2+}$. $^{31}P\{^1H\}$ NMR, δ 19.7 [br m, ^1J(PtP) 3050 and 2942].

Synthesis of $[Pt_2\{\mu\text{-}SCH_2C(O)Ph\}(\mu\text{-}SBu)(PPh_3)_3Br]PF_6$ $\mathbf{10}\cdot PF_6$

1-Bromobutane (1 mL, large excess) was added to a stirred suspension of $[Pt_2(\mu\text{-}S)_2(PPh_3)_4]$ **1** (100 mg, 0.067 mmol) in methanol (25 mL), and the mixture stirred for 1 h to give a yellow solution. ESI MS indicated complete formation of $[Pt_2(\mu\text{-}S)(\mu\text{-}SBu)(PPh_3)_4]^+$. The volatiles were removed by rotary evaporation, the residue redissolved in methanol (25 mL) and $PhC(O)CH_2Br$ (66 mg, 0.33 mmol) added. After stirring for 48 h the solution was filtered to remove traces of insoluble matter and excess NH_4PF_6 (40 mg, 0.245 mmol) added to the filtrate, followed by water (10 mL) to assist precipitation. The product was filtered, washed with water (40 mL) and diethyl ether (40 mL) and dried under vacuum to give $\mathbf{10}\cdot PF_6$ as a brownish powder (61 mg, 56%). Found: C 47.35; H 3.84. $C_{66}H_{61}BrF_6OP_4Pt_2S_2$ (M_r 1641.36) requires C 48.25; H 3.75%. M.p. 216-218 °C. IR ν_{max} 1681 cm^{-1}. ESI MS *m/z* 1497 (100%), $[Pt_2\{\mu\text{-}SCH_2C(O)Ph\}(\mu\text{-}SBu)(PPh_3)_3Br]^+$.

Crystals suitable for an X-ray diffraction study were obtained by vapour diffusion of diethyl ether into a dichloromethane solution of the complex at room temperature.

Synthesis of $[Pt_2\{\mu\text{-}SCH_2C(O)Ph\}(\mu\text{-}SEt)(PPh_3)_3Br]PF_6$ $\mathbf{11}\cdot PF_6$

Following the procedure for $\mathbf{10}\cdot PF_6$, $[Pt_2(\mu\text{-}S)_2(PPh_3)_4]$ **1** (100 mg, 0.067 mmol) in methanol (25 mL) with bromoethane (1 mL, large excess) and $PhC(O)CH_2Br$ (66 mg, 0.34 mmol), followed by precipitation with NH_4PF_6 (40 mg, 0.245 mmol) gave $\mathbf{11}\cdot PF_6$ as a light brown precipitate (67 mg, 62%). Found: C 46.51; H 3.38. $C_{64}H_{57}BrF_6OP_4Pt_2S_2$ (M_r 1613.33) requires C 47.60; H 3.56%. M.p. 191-194 °C. IR ν_{max} 1689 cm^{-1}. ESI MS *m/z* 1469 (100%), $[Pt_2\{\mu\text{-}SCH_2C(O)Ph\}(\mu\text{-}SEt)(PPh_3)_3Br]^+$.

Crystals suitable for an X-ray diffraction study were obtained by vapour diffusion of diethyl ether into a dichloromethane solution of the complex at room temperature.

X-ray crystal structure determinations

Data for **3**·$(PF_6)_2$, **8**·$(BPh_4)_2$ and **10**·PF_6 were collected on a Bruker Apex II diffractometer equipped with a CCD area detector, using Mo-Kα radiation (λ = 0.71073 Å). SADABS [41] was used for empirical absorption correction. Structures were solved by the direct methods option of SHELXS-97 [42] and the Pt, S and P atoms were located. All other non-hydrogen atoms were located from a series of difference maps. Full-matrix least-squares refinement was based on F_o^2 with all non-hydrogen atoms anisotropic and hydrogen atoms in calculated positions. All calculations were carried out using the SHELX-97 suite of programs. A summary of crystallographic parameters and refinement details is given in Table 6.

Most of the details of the structure of **3**·$(PF_6)_2$ evolved normally on refinement. The asymmetric unit of the refined structure contained the dication $[Pt_2\{\mu\text{-}SCH_2C(O)Ph\}_2(PPh_3)_4]^{2+}$, two PF_6^- anions and CH_2Cl_2. There was a significant residual peak adjacent to Pt(2) which was modelled as a partially disordered occupancy of the Pt(2) site. This refined to 7% occupancy. One molecule of CH_2Cl_2 was well resolved, and residual electron density suggested a less well-defined one. This was included in the refinement with constrained C-Cl bond lengths and refined to 83% occupancy. A final difference map revealed more electron density (*ca*. 3-4 e $Å^{-3}$) in a region with solvent-accessible voids of *ca*. 160 $Å^3$ which was presumably more solvent molecules (possibly a diethyl ether). This could not be successfully modeled, so was not included in the final model. All non-hydrogen atoms were refined anisotropically except for the minor Pt(2) component, and hydrogen atoms were included in calculated positions.

Crystal data for **8**·$(BPh_4)_2$ were acquired and solved by direct methods in space group Cc. The Pt, S and P atoms evolved, followed by all other atoms on refinement. All non-hydrogen atoms were refined anisotropically except C(4) which was very floppy. A

disordered solvent molecule was treated as a disordered chlorine atom of CH_2Cl_2 and included in the final refinement.

The structure of **10**·PF_6 was solved by direct methods and almost all details evolved normally. All atoms except hydrogen atoms were refined anisotropically. At the end of the first refinement, two residual peaks of about 4 e $Å^{-3}$ revealed in solvent-accessible spaces. In the final refinement they were treated and refined as the oxygen atoms of partial water molecules taking into account the hydrogen-bonding distances.

Crystallographic data for **11**·PF_6 were obtained on a Bruker AXS SMART APEX diffractometer equipped with a CCD area detector using Mo-Kα radiation. The SMART program [43] was used for the collection of data frames, indexing reflections, and to determine lattice parameters. SAINT [43] was used for integration of the intensity of reflections and for scaling, and SHELXTL [44] was used for space group and structure determination, refinements, graphics and structure reporting. The structure was refined by full-matrix least-squares on F^2 with anisotropic thermal parameters for non-hydrogen atoms. The asymmetric unit contains a cation $[Pt_2\{\mu\text{-}SCH_2C(O)Ph\}(\mu\text{-}SEt)(PPh_3)_3Br]^+$, one PF_6^- anion and one molecule of CH_2Cl_2. The ethyl group attached to S(2) has large thermal motion; in final refinement cycles it was treated as disordered over two positions.

Supplementary material

Crystallographic data for the structures described in this paper have been deposited with the Cambridge Crystallographic Data Centre, CCDC Nos. 822270 [**3**·$(PF_6)_2$], 822271 [**8**·$(BPh_4)_2$], 822272 [**10**·PF_6] and 822269 [**11**·PF_6]. Copies of the data can be obtained free of charge on application to The Director, CCDC, 12 Union Road, Cambridge CB2 1EZ, UK (Fax: +44-1223-336033; e-mail deposit@ccdc.cam.ac.uk or www: http://www.ccdc.cam.ac.uk).

Acknowledgements

We thank the University of Waikato and the National University of Singapore (NUS) for financial support of this work. We also thank Dr. Tania Groutso (University of Auckland) for collection of the X-ray data sets of **3**·$(PF_6)_2$, **8**·$(BPh_4)_2$ and **10**·PF_6 and Lip Lin Koh, Geok Kheng Tan and Yimain Hong (NUS) for the data set of **11**·PF_6.

Table 1 Selected bond lengths (Å) and angles (°) for $[Pt_2\{\mu\text{-}SCH_2C(O)Ph\}_2(PPh_3)_4](PF_6)_2$ **3**·$(PF_6)_2$ with estimated standard deviations in parentheses.

Pt(1)-P(2)	2.2902(14)	Pt(1)-S(1)	2.3917(16)
Pt(1)-P(1)	2.2871(16)	Pt(1)-S(2)	2.3681(15)
Pt(2)-P(3)	2.2703(19)	Pt(2)-S(1)	2.3562(15)
Pt(2)-P(4)	2.2901(16)	Pt(2)-S(2)	2.3843(18)
C(2)-O(2)	1.215(8)	S(2)-C(1)	1.808(8)
C(10)-O(1)	1.222(9)	S(1)-C(9)	1.817(8)
C(9)-C(10)	1.507(10)	C(1)-C(2)	1.504(10)

S(2)-Pt(1)-S(1)	82.32(6)	Pt(1)-S(1)-Pt(2)	94.81(6)
S(2)-Pt(2)-S(1)	82.72(6)	Pt(2)-S(2)-Pt(1)	94.69(6)
S(2)-C(1)-C(2)	119.5(5)	S(1)-C(9)-C(10)	119.7(5)
O(1)-C(10)-C(9)	123.7(7)	O(2)-C(2)-C(3)	120.2(7)
C(1)-S(2)-Pt(1)	107.5(2)	C(9)-S(1)-Pt(2)	110.4(2)
C(1)-S(2)-Pt(2)	108.0(3)	C(9)-S(1)-Pt(1)	112.2(3)

Table 2 Selected bond lengths (Å) and angles (°) for $[Pt_2\{\mu\text{-}SCH_2C(O)Ph\}(\mu\text{-}SBu)(PPh_3)_4](BPh_4)_2$ **8**·$(BPh_4)_2$ with estimated standard deviations in parentheses.

Pt(1)-P(2)	2.321(3)	Pt(1)-S(1)	2.347(3)
Pt(1)-P(1)	2.294(3)	Pt(1)-S(2)	2.383(3)
Pt(2)-P(3)	2.303(3)	Pt(2)-S(1)	2.380(3)
Pt(2)-P(4)	2.284(3)	Pt(2)-S(2)	2.371(3)
S(2)-C(5)	1.830(8)	C(6)-O(1)	1.250(12)
S(1)-C(1)	1.829(10)		

S(2)-Pt(1)-S(1)	82.14(11)	Pt(1)-S(1)-Pt(2)	92.54(11)
S(2)-Pt(2)-S(1)	81.67(11)	Pt(2)-S(2)-Pt(1)	91.86(11)
S(1)-C(1)-C(2)	110.8(7)	O(1)-C(6)-C(5)	119.9(5)
C(6)-C(5)-S(2)	125.6(3)	C(1)-S(1)-Pt(1)	106.0(3)
C(5)-S(2)-Pt(2)	107.9(3)	C(1)-S(1)-Pt(2)	112.3(4)
C(5)-S(2)-Pt(1)	102.7(3)		

Table 3 Selected bond lengths (Å) and angles (°) for $[Pt_2\{\mu\text{-}SCH_2C(O)Ph\}(\mu\text{-}SBu)(PPh_3)_3Br]PF_6$ **10**·PF_6 with estimated standard deviations in parentheses.

Pt(2)-P(2)	2.270(2)	Pt(2)-S(1)	2.3637(19)
Pt(1)-P(1)	2.268(2)	Pt(2)-S(2)	2.3823(19)
Pt(2)-P(3)	2.302(2)	Pt(1)-S(1)	2.2795(18)
Pt(1)-S(2)	2.375(2)	Pt(1)-Br(1)	2.4641(9)
C(2)-C(3)	1.497(11)	S(1)-C(1)	1.824(8)
C(1)-C(2)	1.507(11)	S(2)-C(9)	1.830(8)
C(2)-O(1)	1.220(10)		

S(2)-Pt(1)-S(1)	79.55(7)	Pt(1)-S(1)-Pt(2)	87.78(6)
S(2)-Pt(2)-S(1)	77.74(7)	Pt(2)-S(2)-Pt(1)	85.19(7)
C(1)-S(1)-Pt(1)	109.2(3)	C(9)-S(2)-Pt(2)	120.8(3)
C(1)-S(1)-Pt(2)	104.0(3)	C(9)-S(2)-Pt(1)	114.8(3)
S(1)-Pt(1)-P(1)	93.63(7)	S(2)-Pt(1)-Br(1)	96.22(5)
P(1)-Pt(1)-Br(1)	90.47(5)	P(2)-Pt(2)-P(3)	98.04(7)
P(2)-Pt(2)-S(1)	88.00(7)	P(3)-Pt(2)-S(2)	98.20(7)
S(1)-C(1)-C(2)	110.8(6)	S(2)-C(9)-C(10)	109.0(6)

Table 4 Selected bond lengths (Å) and angles (°) for $[Pt_2\{\mu\text{-}SCH_2C(O)Ph\}(\mu\text{-}SEt)(PPh_3)_3Br]PF_6$ **11**·PF_6 with estimated standard deviations in parentheses.

Pt(1)-P(2)	2.2729(11)	Pt(1)-S(1)	2.3655(10)
Pt(1)-P(1)	2.2992(11)	Pt(1)-S(2)	2.3725(11)
Pt(2)-P(3)	2.2669(11)	Pt(2)-S(1)	2.2799(11)
Pt(2)-Br(1)	2.4657(5)	Pt(2)-S(2)	2.3702(11)
C(1)-C(2)	1.508(6)	C(2)-C(3)	1.492(6)
C(2)-O(1)	1.198(6)	S(1)-C(1)	1.821(4)
S(2)-Pt(1)-S(1)	77.36(4)	S(1)-Pt(2)-P(3)	93.45(4)
S(2)-Pt(2)-S(1)	79.08(4)	Pt(1)-S(1)-Pt(2)	87.52(4)
S(1)-C(1)-C(2)	111.6(3)	Pt(2)-S(2)-Pt(1)	85.30(3)
C(1)-S(1)-Pt(1)	105.24(15)	O(1)-C(2)-C(3)	121.7(4)
C(1)-S(1)-Pt(2)	108.24(16)	S(2)-Pt(2)-Br(1)	96.16(3)

Table 5 A comparison of selected structural parameters of the dialkylated derivatives $[Pt_2\{\mu\text{-}SCH_2C(O)Ph\}_2(PPh_3)_4](PF_6)_2$ **3**·$(PF_6)_2$, $[Pt_2\{\mu\text{-}SCH_2C(O)Ph\}(\mu\text{-}SBu)(PPh_3)_4](BPh_4)_2$ **8**·$(BPh_4)_2$, $[Pt_2\{\mu\text{-}SCH_2C(O)Ph\}(\mu\text{-}SBu)(PPh_3)_3Br]PF_6$ **10**·PF_6 and $[Pt_2\{\mu\text{-}SCH_2C(O)Ph\}(\mu\text{-}SEt)(PPh_3)_3Br]PF_6$ **11**·PF_6

	3·$(PF_6)_2$	**8**·$(BPh_4)_2$	**10**·PF_6	**11**·PF_6
Parameter				
Pt···Pt (Å)	3.4952(5)	3.4159(4)	3.2197(4)	3.2134(2)
S···S (Å)	3.133(2)	3.107(4)	2.979(3)	2.961(1)
Pt-S-Pt (average, °)	94.75(6)	92.20(11)	86.49(7)	86.41(4)
Dihedral angle (°)[†]	156.36	145.11	124.66	123.84

[†]Angle between the $Pt(1)S_2$ and $Pt(2)S_2$ planes

Table 6 Crystal data and structure refinement details for the complexes $[Pt_2\{\mu\text{-}SCH_2C(O)Ph\}_2(PPh_3)_4](PF_6)_2$ **3**·$(PF_6)_2$, $[Pt_2\{\mu\text{-}SCH_2C(O)Ph\}(\mu\text{-}SBu)(PPh_3)_4](PF_6)_2$ **8**·$(BPh_4)_2$, $[Pt_2\{\mu\text{-}SCH_2C(O)Ph\}(\mu\text{-}SBu)(PPh_3)_3Br]PF_6$ **10**·PF_6, and $[Pt_2\{\mu\text{-}SCH_2C(O)Ph\}(\mu\text{-}SEt)(PPh_3)_3Br]PF_6$ **11**·PF_6

	3·$(PF_6)_2$·$2CH_2Cl_2$	**8**·$(BPh_4)_2$·CH_2Cl_2	**10**·PF_6·$2H_2O$	**11**·PF_6·CH_2Cl_2
Formula	$C_{90}H_{78}Cl_4F_{12}O_2P_6Pt_2S_2$	$C_{133}H_{118}B_2Cl_2OP_4Pt_2S_2$	$C_{66}H_{63}BrF_6O_2P_4Pt_2S_2$	$C_{65}H_{59}BrCl_2F_6OP_4Pt_2S_2$
Formula weight	2201.44	2402.97	1660.25	1699.11
Temperature (K)	93(2)	89(2)	89(2)	223(2)
Crystal system	Triclinic	Monoclinic	Monoclinic	Monoclinic
Space group	P-1	Cc	$P2_1/c$	$P2_1/c$
a (Å)	13.9856(5)	31.9776(4)	13.8278(4)	13.9445(6)
b (Å)	17.5866(6)	14.7512(2)	22.7551(7)	22.6725(11)
c (Å)	18.9340(6)	27.7611(4)	19.8603(6)	20.0422(9)
α (°)	91.906(2)	90	90	90
β (°)	101.551(2)	115.730(1)	92.221(2)	90.415(1)
γ (°)	93.392(2)	90	90	90
Volume ($Å^3$)	4549.8(3)	11796.7(3)	6244.4(3)	6336.3(5)

Z	2	4	4	4
Calculated density (g cm^{-3})	1.607	1.353	1.766	1.781
Absorption coefficient (mm^{-1})	3.411	2.554	5.347	5.352
F(000)	2176	4864	3248	3312
Crystal size (mm^3)	0.29 x 0.27 x 0.15	0.25 x 0.22 x 0.20	0.28 x 0.22 x 0.20	0.46 x 0.26 x 0.10
Reflections collected /unique	106616/21940 [R_{int} 0.0448]	73575/25367 [R_{int} 0.0305]	74187/14958 [R_{int} 0.0680]	44741/14543 [R_{int} 0.0435]
Absorption correction	Semi-empirical from equivalents	Semi-empirical from equivalents	Semi-empirical from equivalents	Semi-empirical from equivalents
Max. and min. transmission	0.6286 and 0.4379	0.6292 and 0.5677	0.4144 and 0.3159	0.6166 and 0.1921
Data / restraints / parameters	21940 / 20 / 1069	25367 / 301 / 1306	14958 / 0 / 748	14543 / 2 / 744
GoF (on F^2)	1.110	1.055	1.199	1.004
Final R indices [$I > 2\sigma(I)$]	R_1 0.0500, wR_2 0.1252	R_1 0.0439, wR_2 0.1362	R_1 0.0505, wR_2 0.0960	R_1 0.0351, wR_2 0.0792
R indices (all data)	R_1 0.0709, wR_2 0.1403	R_1 0.0538, wR_2 0.1450	R_1 0.0914, wR_2 0.1090	R_1 0.0474, wR_2 0.0835
Largest diff. peak and hole (e $Å^{-3}$)	3.562 and -1.439	3.279 and -0.997	1.812 and -2.637	1.575 and -0.583

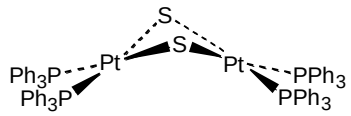

1

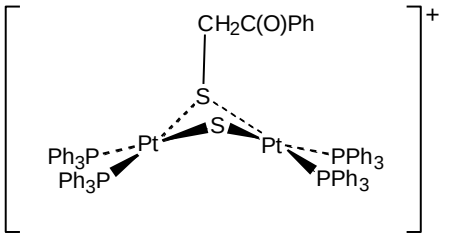

2

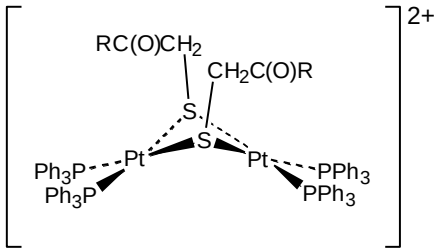

3, R = Ph
5, R = Pyr
7, R = Cou

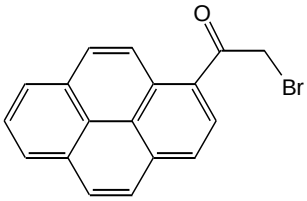

PyrC(O)CH_2Br, **4**

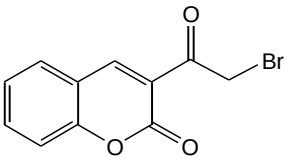

CouC(O)CH_2Br, **6**

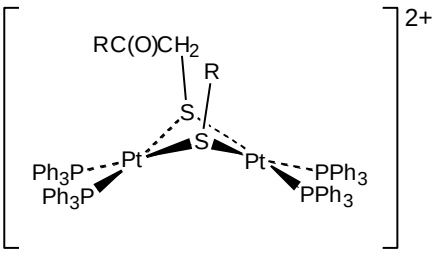

8, R = n-Bu
9, R = Et

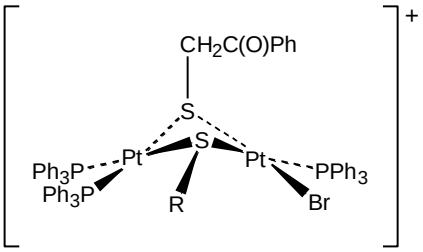

10, R = n-Bu
11, R = Et

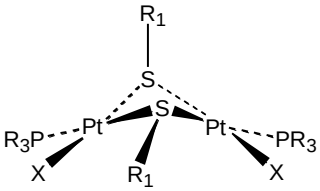

12a, R_3P = PPh_3, R_1 = Me, X = NO_2
12b, R_3P = PMe_2Ph, R_1 = CH_2Ph, X = SCH_2Ph
12c, R_3P= PPr_3, R_1 = Et, X = Cl
12d, R_3P = PPh_3, R_1 = Me, X = Br

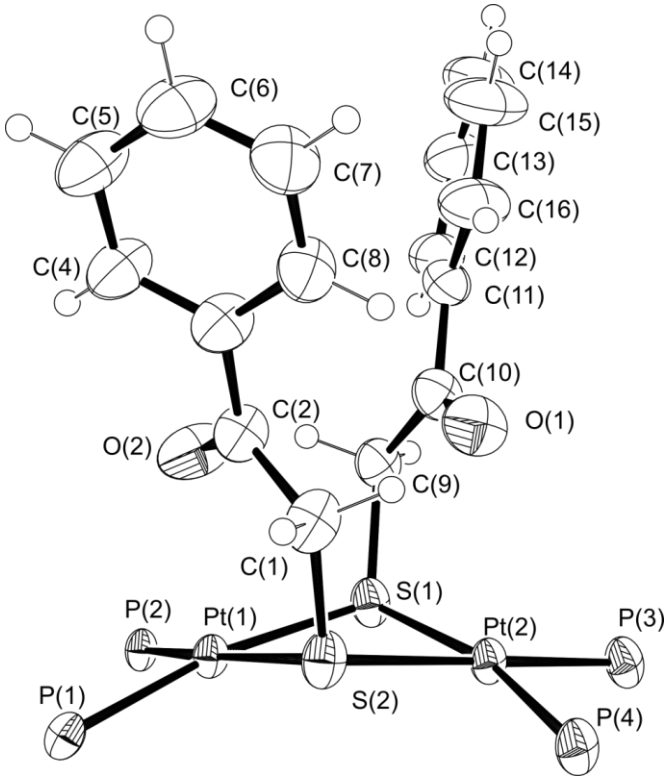

Figure 1 Molecular structure of the cation of $[Pt_2\{\mu\text{-}SCH_2C(O)Ph\}_2(PPh_3)_4](PF_6)_2$ **3**·$(PF_6)_2$ showing the atom numbering scheme, with thermal ellipsoids at the 50% probability level. Phenyl rings of the PPh_3 ligands are omitted for clarity.

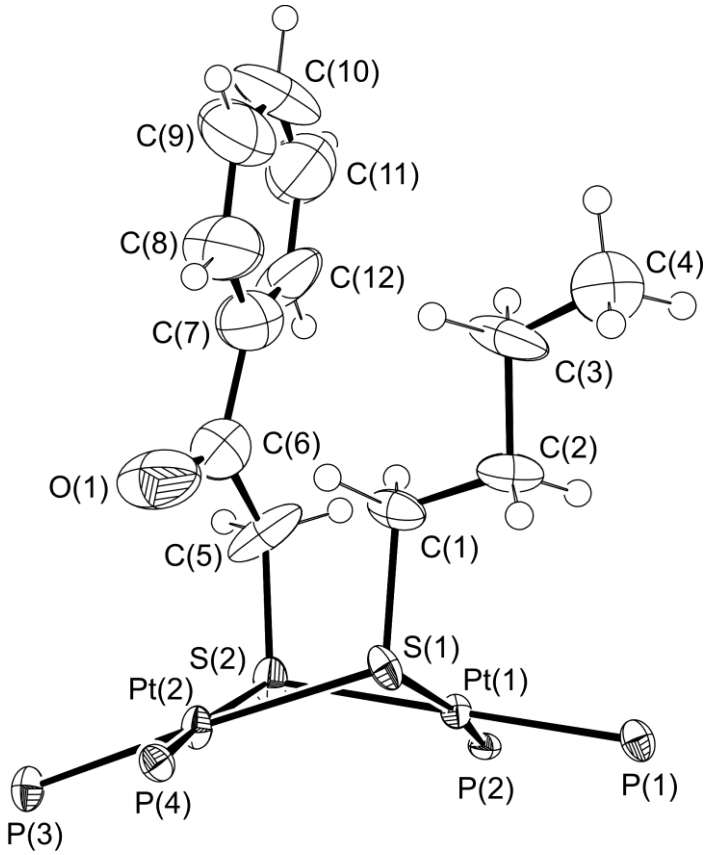

Figure 2 Molecular structure of the cation of $[Pt_2\{\mu\text{-}SCH_2C(O)Ph\}(\mu\text{-}SBu)(PPh_3)_4](BPh_4)_2$ **8**·$(BPh_4)_2$ showing the atom numbering scheme, with thermal ellipsoids at the 50% probability level. Phenyl rings of the PPh_3 ligands are omitted for clarity.

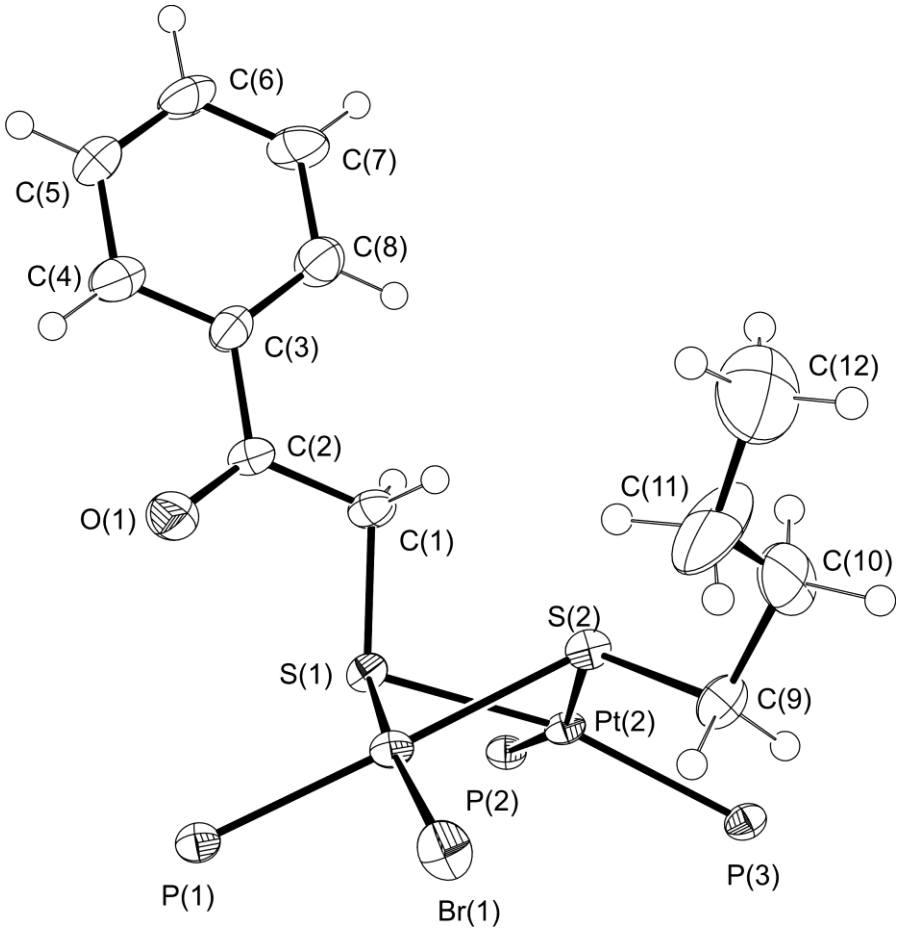

Figure 3 Molecular structure of the cation of $[Pt_2\{\mu\text{-}SCH_2C(O)Ph\}(\mu\text{-}SBu)(PPh_3)_3Br]PF_6$ **10**·PF_6 showing the atom numbering scheme, with thermal ellipsoids at the 50% probability level. Phenyl rings of the PPh_3 ligands are omitted for clarity.

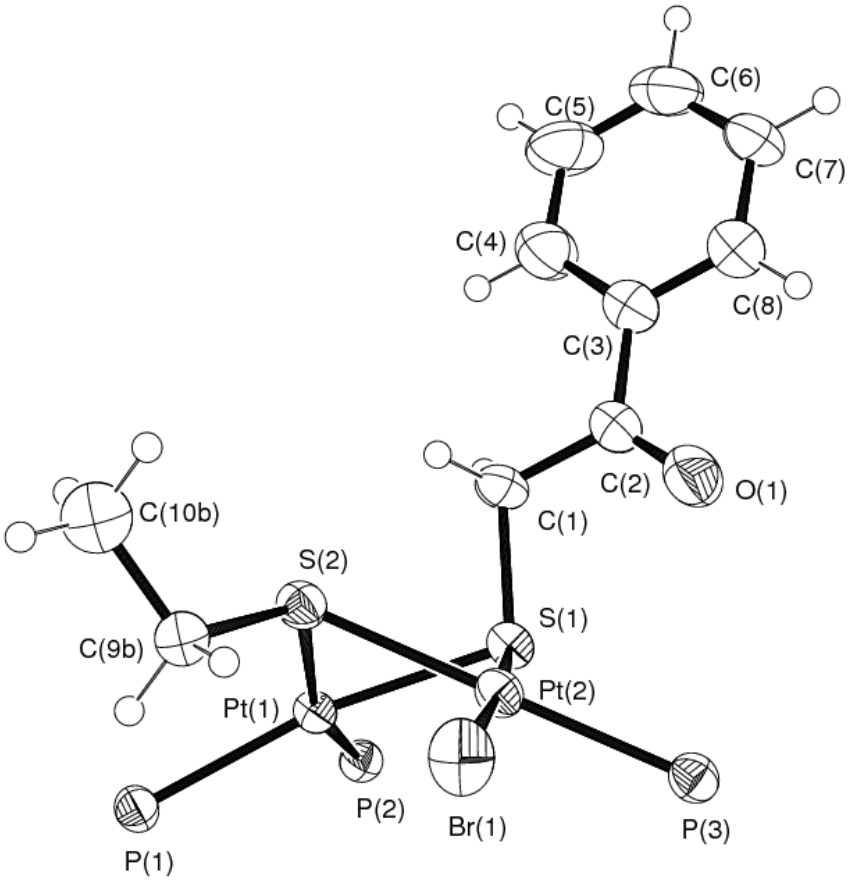

Figure 4 Molecular structure of the cation of $[Pt_2\{\mu\text{-}SCH_2C(O)Ph\}(\mu\text{-}SEt)(PPh_3)_3Br]PF_6$ **11**·PF_6 showing the atom numbering scheme, with thermal ellipsoids at the 50% probability level. Phenyl rings of the PPh_3 ligands are omitted for clarity.

References

[1] J. Chatt and D. M. P. Mingos, J. Chem. Soc. A (1970) 1243

[2] R. Ugo, G. La Monica, S. Cenini, A. Segre and F. Conti, J. Chem. Soc. A (1971) 522

[3] R. R. Gukathasan, R. H. Morris and A. Walker, Can. J. Chem. 61 (1983) 2490

[4] C. E. Briant, C. J. Gardner, T. S. A. Hor, N. D. Howells and D. M. P. Mingos, J. Chem. Soc., Dalton Trans. (1984) 2645

[5] S.-W. A. Fong and T. S. A. Hor, J. Chem. Soc., Dalton Trans. (1999) 639

[6] T. S. A. Hor, J. Cluster Sci. 7 (1996) 263

[7] P. González-Duarte, A. Lledós and R. Mas-Ballesté, Eur. J. Inorg. Chem. (2004) 3585

[8] A. Bencini, M. Di Vaira, R. Morassi, P. Stoppioni and F. Mele, Polyhedron 15 (1996) 2079

[9] J. S. L. Yeo, G. Li, W.-H. Yip, W. Henderson, T. C. W. Mak and T. S. A. Hor, J. Chem. Soc., Dalton Trans. (1999) 435

[10] G. Li, C.-K. Lam, S. W. Chien, T. C. W. Mak and T. S. A. Hor, J. Organomet. Chem. 690 (2005) 990

[11] A. Nova, P. González-Duarte, A. Lledós, R. Mas-Ballesté and G. Ujaque, Inorg. Chim. Acta 359 (2006) 3736

[12] W. Henderson, G. C. Saunders and T. S. A. Hor, Inorg. Chim. Acta 368 (2011) 6

[13] A. Nova, R. Mas-Ballesté, G. Ujaque, P. González-Duarte and A. Lledós, Chem. Commun. (2008) 3130

[14] W. Henderson, S. H. Chong and T. S. A. Hor, Inorg. Chim. Acta 359 (2006) 3440

[15] F. Novio, R. Mas-Ballesté, I. Gallardo, P. González-Duarte, A. Lledós and N. Vila, Dalton Trans. (2005) 2742

[16] R. Mas-Ballesté, M. Capdevila, P. A. Champkin, W. Clegg, R. A. Coxall, A. Lledós, C. Mégret and P. González-Duarte, Inorg. Chem. 41 (2002) 3218

[17] A. Nova, R. Mas-Ballesté, G. Ujaque, P. González-Duarte and A. Lledós, Dalton Trans. (2009) 5980

[18] B. J. Deadman, W. Henderson, B. K. Nicholson, L. E. Petchell, S. L. Rose and T. S. A. Hor, Inorg. Chim. Acta 363 (2010) 637

[19] J. S. L. Yeo, J. J. Vittal and T. S. A. Hor, Eur. J. Inorg. Chem. (2003) 277

[20] J. S. L. Yeo, J. J. Vittal, W. Henderson and T. S. A. Hor, Organometallics 21 (2002) 2944

[21] J. Li, F. Li, L. L. Koh and T. S. A. Hor, Dalton Trans. 39 (2010) 2441

[22] O. T. Ujam, S. M. Devoy, W. Henderson, B. K. Nicholson and T. S. A. Hor, Inorg. Chim. Acta 363 (2010) 3558

[23] S. H. Chong, W. Henderson and T. S. A. Hor, Dalton Trans. (2007) 4008

[24] S. H. Chong, W. Henderson and T. S. A. Hor, Eur. J. Inorg. Chem. (2007) 4958

[25] S. M. Devoy, W. Henderson, B. K. Nicholson and T. S. A. Hor, Inorg. Chim. Acta 363 (2010) 25

[26] S. M. Devoy, W. Henderson, B. K. Nicholson and T. S. A. Hor, Inorg. Chim. Acta 362 (2009) 1194

[27] S. H. Chong, D. J. Young and T. S. A. Hor, J. Organomet. Chem. 691 (2006) 349

[28] S. H. Chong, L. L. Koh, W. Henderson and T. S. A. Hor, Chem. Asian J. (2006) 264

[29] S. H. Chong, D. J. Young and T. S. A. Hor, Chem. Asian J. 2 (2007) 1356

[30] Cambridge Structural Database http://www.ccdc.cam.ac.uk/products/csd/radii/

[31] T. G. Appleton, H. C. Clark and L. E. Manzer, Coord. Chem. Rev. 10 (1973) 335

[32] W. Henderson, B. K. Nicholson, S. M. Devoy and T. S. A. Hor, Inorg. Chim. Acta 361 (2008) 1908

[33] C. Mendoza, J. Benet-Buchholz, M. A. Pericás and R. Vilar, Dalton Trans. (2009) 2974

[34] P. H. Bird, U. Siriwardane, R. D. Lai and A. Shaver, Can. J. Chem. 60 (1982) 2075; CSD ref: BIRJAN

[35] M. C. Hall, J. A. J. Jarvis, B. T. Kilbourn and P. G. Owston, J. Chem. Soc., Dalton Trans. (1972) 1544; CSD refcode ETHPDP

[36] C. Albrecht, S. Schwieger, C. Bruhn, C. Wagner, R. Kluge, H. Schmidt and D. Steinborn, J. Am. Chem. Soc. 129 (2007) 4551; CSD refcode XIDZAM

[37] M. Capdevila, W. Clegg, P. González-Duarte, A. Jarid and A. Lledós, Inorg. Chem. 35 (1996) 490

[38] W. Henderson, S. Thwaite, B. K. Nicholson and T. S. A. Hor, Eur. J. Inorg. Chem. (2008) 5119

[39] L. J. Arnold. J. Chem. Educ. 69 (1992) 811

[40] http://fluorine.ch.man.ac.uk/research/tools.php

[41] R. H. Blessing, Acta Cryst. Sect. A 51 (1995) 33

[42] G. M. Sheldrick, SHELX-97 - Programs for the Solution and Refinement of Crystal Structures, University of Göttingen, Germany, 1997

[43] SMART and SAINT, in Software Reference Manuals, version 4.0, Siemens Energy & Automation Inc., Madison, Wisconsin, USA, 1996

[44] SHELXTL, Version 6.14, Bruker AXS Inc., Madison, Wisconsin, USA, 2000